




Syntheses, structures and properties of four second-sphere coordination complexes via metal halide anion and naphthalene-based ligand

Lei Li, Wen-Long Duan, Jian Tong, Yan-Qing Fu, Rong-Rong Zhang, Ren-Wang Jiang & Fang Guo

To cite this article: Lei Li, Wen-Long Duan, Jian Tong, Yan-Qing Fu, Rong-Rong Zhang, Ren-Wang Jiang & Fang Guo (2015) Syntheses, structures and properties of four second-sphere coordination complexes via metal halide anion and naphthalene-based ligand, Journal of Coordination Chemistry, 68:20, 3566-3579, DOI: [10.1080/00958972.2015.1074683](https://doi.org/10.1080/00958972.2015.1074683)

To link to this article: <http://dx.doi.org/10.1080/00958972.2015.1074683>

 View supplementary material 

 Accepted author version posted online: 29 Jul 2015.
Published online: 17 Aug 2015.

 Submit your article to this journal 

 Article views: 88

 View related articles 

 View Crossmark data 

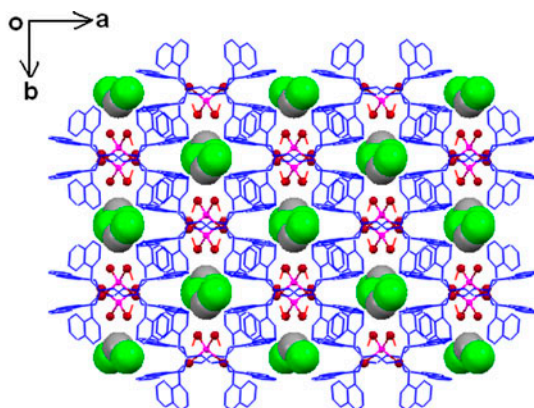
Syntheses, structures and properties of four second-sphere coordination complexes via metal halide anion and naphthalene-based ligand

LEI LI†, WEN-LONG DUAN†, JIAN TONG†, YAN-QING FU†,
RONG-RONG ZHANG‡, REN-WANG JIANG‡ and FANG GUO*†

†College of Chemistry, Liaoning University, Shenyang, China

‡Guangdong Province Key Laboratory of Pharmacodynamic Constituents of TCM and New Drugs Research, College of Pharmacy, Jinan University, Guangzhou, PR China

(Received 4 May 2014; accepted 30 June 2015)



X-shaped host framework formed by second-sphere coordination strategy.

Second-sphere coordination refers to any intermolecular interactions with the ligands directly bound to the primary coordination sphere of a metal ion. Four supramolecular complexes, $0.5[\text{L}\cdot 2\text{H}]^{2+}\cdot 0.5[\text{MCl}_4]^{2-}\cdot [\text{CH}_3\text{OH}]\cdot 0.5[\text{CH}_2\text{Cl}_2]$ ($\text{M} = \text{Co}$, crystal **1**; $\text{M} = \text{Mn}$, crystal **2**), $0.5[\text{L}\cdot 2\text{H}]^{2+}\cdot 0.5[\text{ZnBr}_4]^{2-}\cdot [\text{CH}_3\text{OH}]\cdot 0.5[\text{CH}_2\text{Cl}_2]$ (crystal **3**), and $0.5[\text{L}\cdot 2\text{H}]^{2+}\cdot 0.5[\text{Cu}_2\text{Br}_4]^{2-}\cdot \text{H}_2\text{O}$ (crystal **4**), based on naphthalene-based ligand N,N,N',N' -tetra-*p*-methyl-naphthyl-ethanediamine (**L**), have been synthesized. X-ray analysis reveals that **1**–**3** are isostructural, in which the methanol molecules are bridges, connecting the protonated **L** and metal chloride anions via $\text{N}\cdots\text{H}\cdots\text{O}$ and $\text{O}\cdots\text{H}\cdots\text{Cl}$ (**Br**) interactions to construct the host framework, and forming X-shaped cavity accessible for the inclusion of weakly polar guest molecules of dichloromethane. Dichloromethane is connected with the host framework through van der Waals forces. In **4**, a dinuclear anion $[\text{Cu}_2\text{Br}_4]^{2-}$ is connected with the ligand through $\text{N}\cdots\text{H}\cdots\text{Br}$ interactions, in which the water molecules are accommodated between chains formed by the ligand and $[\text{Cu}_2\text{Br}_4]^{2-}$. Structure stability, thermal analysis, and photoluminescent properties were studied for **1**–**4**.

Keywords: Second-sphere coordination; Inclusion complex; Naphthalene-based ligand

*Corresponding author. Email: fguo@lnu.edu.cn

Introduction

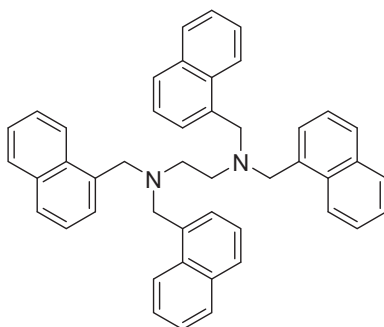
Controlling supramolecular self-assembly through crystal engineering is a way to gain materials with desired properties. Crystal engineering of various molecular components, either organic or mixed metal–organic assembly, through non-covalent interactions was also called “supramolecular synthesis” [1]. Sophisticated supramolecular assemblies based on non-covalent interactions (hydrogen bonding, C–H···O, and C–H··· π weak interactions) [2] can be built [3], and significant advances in areas like molecular transport [4], improved pharmaceutical properties [5], gas adsorption [6], and semiconductors [7] have been witnessed. Employing non-covalent interactions cooperatively with metal salts or metal ligation to form coordination solids has also received attention [8]. The use of organic cations and metal ions via second-sphere coordination to construct frameworks with accessible voids/spaces for inclusion of guest molecules is an interesting field, first mentioned by Colquhoun *et al.* [9], and more recently has been exploited by Beauchamp and Loeb [10]. In general, the construction of second-sphere coordination refers to any intermolecular interactions with the ligands directly bound to the primary coordination sphere of a metal ion. Based on this strategy, some urea(amido)-containing ligands have been applied as extractants for highly selective extraction of $[\text{PtCl}_6]^{2-}$, $[\text{ZnCl}_4]^{2-}$ and $[\text{CoCl}_4]^{2-}$, and more recently using α -cyclodextrin for gold recovery [11, 12]. Second-sphere coordination was also exploited in anion recognition and binding [13]. We recently reported the solid-state mechanochemical dehydrohalogenation reaction starting from salts assembled by second-sphere coordination [14].

Our research has been interested in constructing hydrogen-bonded networks through second coordination sphere interactions of metal complexes [15], herein, we have designed a naphthalene-based ligand, which can act as a fluorescence chemosensor, N,N,N',N'-tetra-*p*-methyl-naphthyl-ethanediamine (**L**, scheme 1). **L** can be doubly protonated and coordinated with the “first-sphere” of $[\text{MX}_4]^{2-}$ to form four supramolecular complexes, $0.5[\text{L}\cdot 2\text{H}]^{2+}\cdot 0.5[\text{MCl}_4]^{2-}\cdot [\text{CH}_3\text{OH}]\cdot 0.5[\text{CH}_2\text{Cl}_2]$ (M = Co, crystal **1**; Mn, crystal **2**), $0.5[\text{L}\cdot 2\text{H}]^{2+}\cdot 0.5[\text{ZnBr}_4]^{2-}\cdot [\text{CH}_3\text{OH}]\cdot 0.5[\text{CH}_2\text{Cl}_2]$ (crystal **3**), and $0.5[\text{L}\cdot 2\text{H}]^{2+}\cdot 0.5[\text{Cu}_2\text{Br}_4]^{2-}\cdot \text{H}_2\text{O}$ (crystal **4**). In **1**–**3**, the MeOH as bridge, connects the protonated ligand and $[\text{MCl}_4]^{2-}$ through N–H···O and O–H···Cl interactions simultaneously, forming the host framework, in which an X-shaped channel was formed accessible for the inclusion of weakly polar guest molecules, such as dichloromethane. Crystal **4** forms a different structure from **1**–**3**, and water molecules are included in the structure. The anions $[\text{MX}_4]^{2-}$ acting as an “off-on” switching template can affect the fluorescence properties.

Experimental

Materials and instrumentation

All chemicals were obtained from commercial sources and used without purification. IR spectra were obtained with a Perkin–Elmer 100 FT-IR spectrometer (USA) using KBr pellets. NMR spectra were recorded on a Mercury-Plus 300 spectrometer (VARIAN, 300 MHz) at 25 °C with TMS as the internal reference.



Scheme 1. Structure of L.

Preparation of L

Dibenzylamine (1.7 mL, 25 mmol) was slowly added to the solution of 10-g NaHCO_3 and 20-mL distilled water in a 500-mL flask. 1-Chloromethyl naphthalene (13 mL, 100 mmol) was then continuously (2–3 drops/s) added into the solution. After the reaction was heated to 95 °C and stirred for 4.5 h, the mixture was cooled to room temperature. The reaction product was dissolved in ethyl acetate and then cyclohexane was added dropwise to the solution. The resulting white precipitate was filtered and dried in vacuo, produced white powder 10.5 g, yield 54%. m.p. 209–210 °C; IR(KBr), λ_{max} (cm^{-1}): 3448.44 cm^{-1} (N^+H), 3039.20 cm^{-1} (Ar), 2960.32, 2800.76, 1595.22, 1509.23 cm^{-1} (Ar), 1397.36 cm^{-1} (C–N), 847.19 cm^{-1} (Ar); ^1H NMR (CDCl_3 , 300 MHz) δ : 2.84 (4H, s, CH_2), 3.90 (8H, s, CH_2), 7.16–7.19 (4H, m, Naph-H), 7.26–7.37 (8H, m, Naph-H), 7.39–7.41 (4H, m, Naph-H), 7.69–7.72 (4H, m, Naph-H), 7.77–7.79 (4H, m, Naph-H), 7.85–7.88 (4H, m, Naph-H). Elemental analysis (%), calculated for $\text{C}_{46}\text{H}_{40}\text{N}_2$: C, 89.03; H, 6.45; N, 4.52. Found: C, 88.91; H, 6.50; N, 4.56.

L (0.01 g, 0.016 mmol), 5 mL of dichloromethane, and 5 mL of methanol were placed in a 50-mL Erlenmeyer flask and shaken until the contents were dissolved. The flask was allowed to stand for over 3 days at room temperature. Recrystallization produced colorless block crystals. Yield 84%. m.p. 209–210 °C.

Preparation of $0.5[\text{L}\cdot 2\text{H}]^{2+}\cdot 0.5[\text{CoCl}_4]^{2-}\cdot [\text{CH}_3\text{OH}]\cdot 0.5[\text{CH}_2\text{Cl}_2]$ (1)

L (0.01 g, 0.016 mmol), 5 mL of dichloromethane, $\text{CoCl}_2\cdot 6\text{H}_2\text{O}$ (0.0076 g, 0.032 mmol), 5 mL of methanol, and three drops (0.15 mL) of concentrated hydrochloric acid were placed in a 50-mL Erlenmeyer flask and shaken until the contents were dissolved. The flask was allowed to stand overnight at room temperature. Recrystallization produced blue block crystals. Yield: 0.0124 g. m.p. 248–250 °C. Elemental analysis (%), calculated for $\text{C}_{49}\text{H}_{52}\text{N}_2\text{O}_2\text{CoCl}_6$: C, 60.49; H, 5.35; N, 2.88. Found: C, 60.31; H, 5.45; N, 2.93.

Preparation of $0.5[\text{L}\cdot 2\text{H}]^{2+}\cdot 0.5[\text{MnCl}_4]^{2-}\cdot [\text{CH}_3\text{OH}]\cdot 0.5[\text{CH}_2\text{Cl}_2]$ (2)

L (0.01 g, 0.016 mmol), 5 mL of dichloromethane, $\text{MnCl}_2\cdot 4\text{H}_2\text{O}$ (0.063 g, 0.032 mmol), 5 mL of methanol, and three drops (0.15 mL) of concentrated hydrochloric acid were placed in a 50-mL Erlenmeyer flask and shaken until the contents were dissolved. The flask

was allowed to stand for 3–4 days at room temperature. Recrystallization produced colorless block crystals. Yield: 0.0101 g. m.p. 188–205 °C. Elemental analysis (%), calculated for $C_{49}H_{52}N_2O_2MnCl_6$: C, 60.74; H, 5.37; N, 2.89. Found: C, 60.70; H, 5.47; N, 2.91.

Preparation of $0.5[L\cdot 2H]^{2+}\cdot 0.5[ZnBr_4]^{2-}\cdot [CH_3OH]\cdot 0.5[CH_2Cl_2]$ (3)

L (0.01 g, 0.016 mmol), 5 mL of dichloromethane, zinc bromide (0.0072 g, 0.032 mmol), 5 mL of methanol, and three drops (0.15 mL) of concentrated hydrobromic acid were placed in a 50-mL Erlenmeyer flask and shaken until the contents were dissolved. The flask was allowed to stand for 2–3 days at room temperature. Recrystallization produced colorless block crystals. Yield: 0.0134 g. m.p. 188–190 °C. Elemental analysis (%), calculated for $C_{49}H_{52}N_2O_2ZnBr_4Cl_2$: C, 50.84; H, 4.50; N, 2.42. Found: C, 50.78; H, 4.54; N, 2.48.

Preparation of $0.5[L\cdot 2H]^{2+}\cdot 0.5[Cu_2Br_4]^{2-}\cdot H_2O$ (4)

L (0.01 g, 0.016 mmol), 5 mL of dichloromethane, copper bromide (0.0071 g, 0.032 mmol), 5 mL of methanol, and three drops (0.15 mL) of concentrated hydrobromic acid were placed in a 50-mL Erlenmeyer flask and shaken until the contents were dissolved. The flask was allowed to stand for 2–3 days at room temperature, producing dark brown block crystals. Yield: 0.0137 g. m.p. 188–189 °C. Elemental analysis (%), calculated for $C_{46}H_{46}N_2O_2Cu_2Br_4$: C, 49.94; H, 4.16; N, 2.53. Found: C, 49.80; H, 4.21; N, 2.56.

Crystallography

Crystal structure data were collected on a Bruker P4 diffractometer with Mo $K\alpha$ radiation ($\lambda = 0.71073$ Å). The structures were determined using direct methods and refined (based on F^2 using all independent data) by full-matrix least-square methods (SHELXTL 97). Data were reduced using the Bruker SAINT software. All non-hydrogen atoms were directly located from difference Fourier maps and refined anisotropically with SHELXTL. The molecules of dichloromethane and methanol were well resolved, but the thermal displacement parameters of some atoms are relatively large, partly owing to the loose packing in the void and partly because the atomic positions represent an average between the included guest molecules. Hydrogens of ligand were generated geometrically and located from difference maps. The hydrogens of water molecules were not successfully located from difference maps due to the disorder of water. The details of data collection, data reduction, and crystallographic data are summarized in Supporting Information, table S1 (see online supplemental material at <http://dx.doi.org/10.1080/00958972.2015.1074683>). CCDC 999407, 999408, 999409, 999411, and 999412 contain the supplementary crystallographic data for this article.

Fluorescence measurements

Solid-state emission spectra were recorded for solid samples which were loaded into a sample cell (1 cm diameter), which was then fixed on a bracket at room temperature with a Hitachi F-7000 fluorescence spectrophotometer. The excitation and emission slits used for the measurement of the solid state of the crystals were 2.5 nm wide, the scan speed was 1200 nm min^{-1} , and the scan voltage was 700 V.

Results and discussion

Structure of **L**

L crystallized in *P*-1 space group with half molecule in one asymmetric unit. The structure was stabilized by C–H $\cdots\pi$ interaction between naphthalene rings of neighboring **L** molecules [C3–H3 \cdots Cg (centroid of naphenyl ring C14–C23: 3.893 Å, 154.2°; the shortest distance is C3–H3 \cdots C17: 3.699 Å, 146.7°), as seen in figure 1.

Structure of **1** and **2**

Single crystals of the outer-sphere complexes, $0.5[\mathbf{L}\cdot 2\mathbf{H}]^{2+}\cdot 0.5[\text{MCl}_4]^{2-}\cdot [\text{CH}_3\text{OH}]\cdot 0.5[\text{CH}_2\text{Cl}_2]$ (M = Co, Crystal **1**; M = Mn, crystal **2**), were readily achieved by mixing solution of metal chloride in MeOH and a HCl/MeOH/dichloromethane solution of **L**. **1** and **2** were measured by powder X-ray diffraction (PXRD), showing well-overlapped peaks with their simulated PXRD patterns, suggesting good correlation of the crystal structures with the bulk materials (Supporting Information).

X-ray analysis revealed that **1** and **2** are isostructural. The structures crystallize as monoclinic *C*2/*c* space group and there are half dianion $[\text{MCl}_4]^{2-}$, half doubly protonated **L**, half dichloromethane molecule, and one methanol molecule in each asymmetric unit [figure 2(a)].

The metal atom in **1** and **2** exhibits highly distorted tetrahedral coordination environment with Co–Cl bond lengths of 2.300(5)–2.328(3) Å and Cl–Co–Cl bond angles of 106.21(19)°–112.46(18)° in $[\text{CoCl}_4]^{2-}$ of crystal **1**; Mn–Cl bond lengths of 2.341(7)–2.376(7) Å, and Cl–Mn–Cl bond angles of 106.85(4)°–112.65(2)° in $[\text{MnCl}_4]^{2-}$ of crystal **2**.

The doubly protonated **L** is a divalent cation. The included methanol guest molecules are bridges, connecting **L** and $[\text{MCl}_4]^{2-}$ (M = Co, Mn). First, the protonated NH of **L** as hydrogen bonding donor is connected with hydroxyl group of methanol through N–H \cdots O interaction (i) (2.844 Å, 159.80° in **1**; 2.799 Å, 163.46° in **2**), and then the same methanol as hydrogen bonding donor links the $[\text{MCl}_4]^{2-}$ anion through O–H \cdots Cl interaction, (ii) (3.253 Å, 161.31° in **1**; 3.194 Å, 159.02° in **2**). Thus, one dianion $[\text{MCl}_4]^{2-}$ (M = Co, Mn) is connected with two protonated **L** using methanol bridges. The above units are expanded into a 1-D hydrogen-bonded chain along the *c*-axis [figure 2(b)].

Adjacent 1-D chains are linked through C–H \cdots Cl interactions (3.691 Å, 159.31° in **1**; 3.705 Å, 141.94° in **2**) between naphthalene ring and $[\text{MCl}_4]^{2-}$ (M = Co, Mn), constructing an X-shaped host framework [figure 2(c)], which is available for dichloromethane guest molecules. Examination of the extended structure along the *c*-axis revealed that channels with approximate dimensions of 8.5 Å \times 4.3 Å exist, within which dichloromethane molecules are connected with the framework through van der Waals interactions (the nearest distance between dichloromethane and host framework is 3.817 Å).

Structure of **3**

Hydrogen bonding strength of N–H \cdots Cl is stronger than N–H \cdots Br, so we are interested to study the effect of the anion on the formation of isostructural materials. We have crystallized **L** with $[\text{ZnBr}_4]^{2-}$ using the same protocol as for **1** and **2**, producing $0.5[\mathbf{L}\cdot 2\mathbf{H}]^{2+}\cdot 0.5[\text{ZnBr}_4]^{2-}\cdot [\text{CH}_3\text{OH}]\cdot 0.5[\text{CH}_2\text{Cl}_2]$ (**3**). The experimental PXRD pattern of **3** and simulated PXRD pattern are well matched, as seen in Supporting Information. Single crystal X-ray

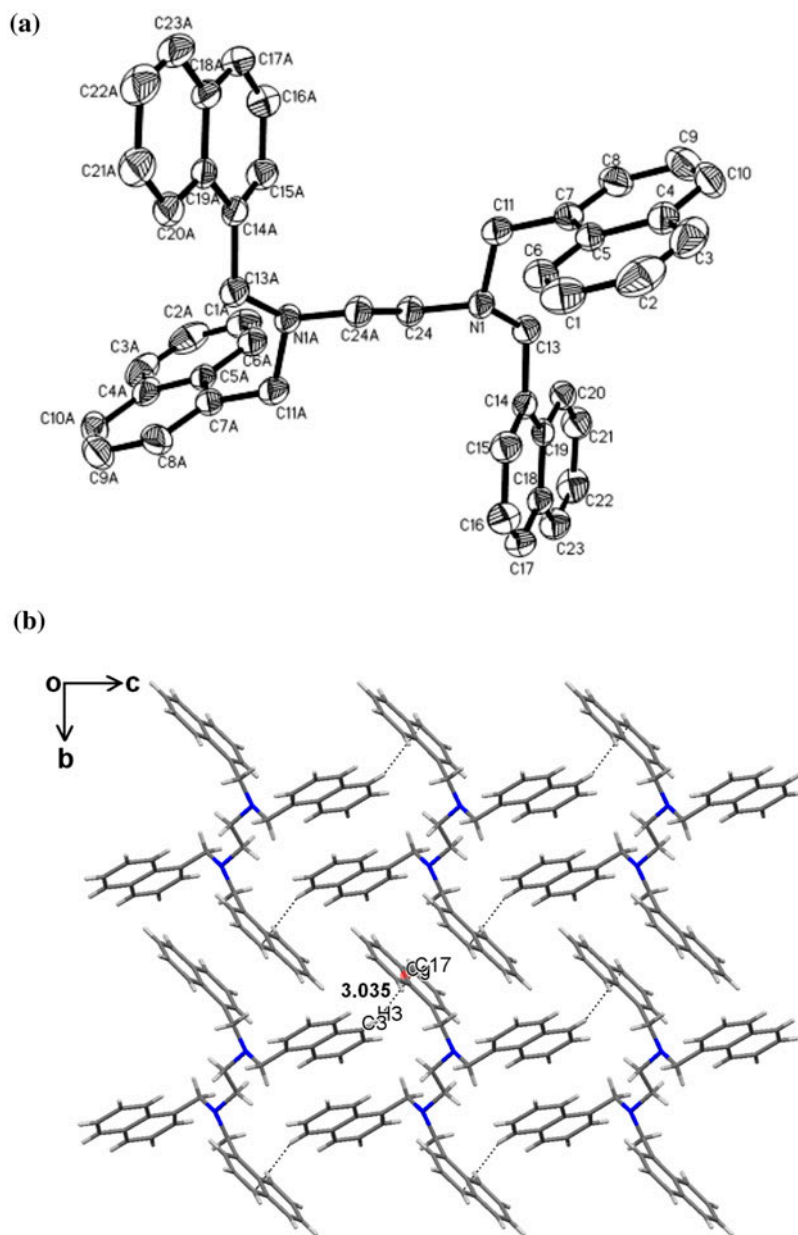


Figure 1. (a) The 30% probability ellipsoids in the ORTEPs for **L** and (b) Structural packing along the *a*-axis.

diffraction clearly shows that the crystal structure is isostructural to **1** and **2** (Supporting Information). $[\text{ZnBr}_4]^{2-}$ forms a distorted tetrahedron with Zn–Br bond lengths of 2.379 (3)–2.417(3) Å and Br–Zn–Br bond angles of 106.76(14)°–113.09(11)°. The N–H \cdots O (2.780 Å, 150.66°) and O–H \cdots Br (3.351 Å, 151.65°) hydrogen bonding stabilizes the structure. The change in the anion interaction for **3** does not affect the crystal packing.

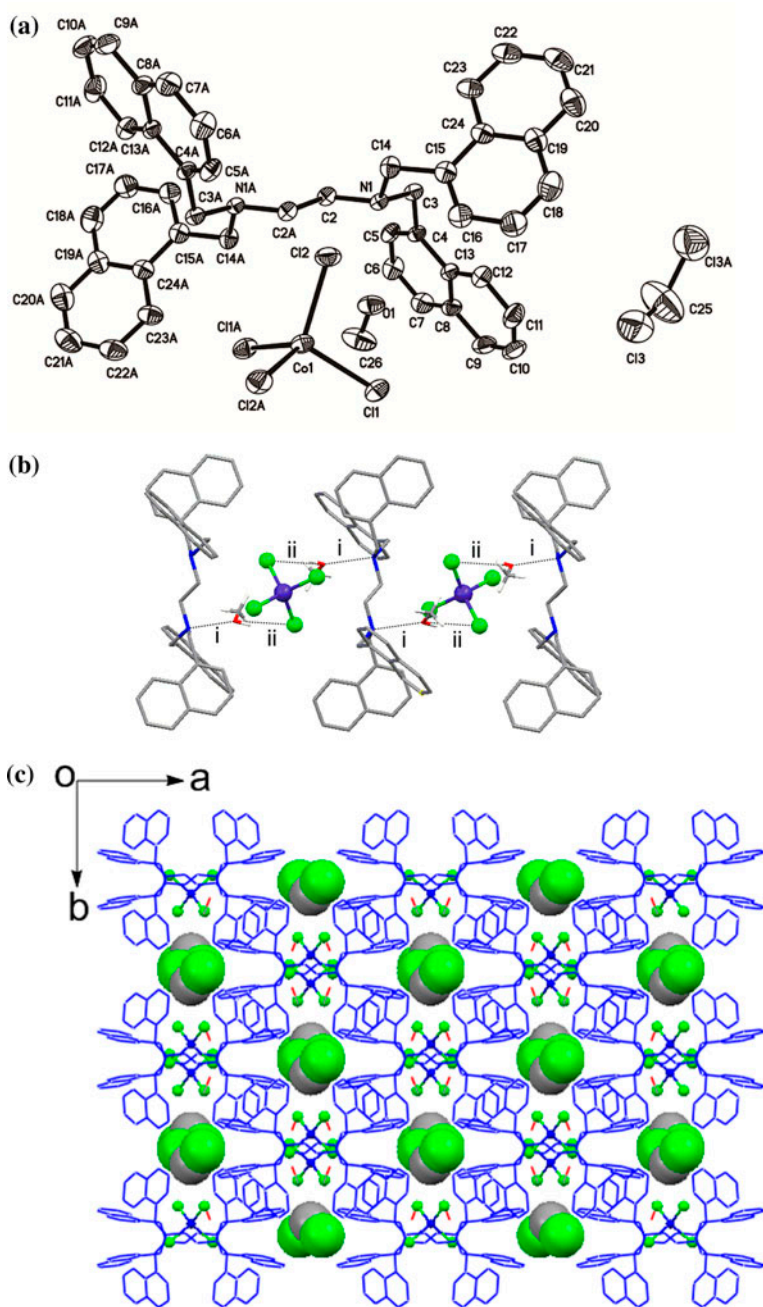


Figure 2. (a) The 20% probability ellipsoids in the ORTEPs for **1**, (b) 1-D hydrogen-bonded chain formed by [CoCl₄]²⁻ and protonated L¹ using methanol as bridges, N-H...O interaction (i) and O-H...Cl interaction (ii), and (c) The structural packing along the *c*-axis, with the formation of host framework accessible for the dichloromethane guest molecules. Crystals **2** and **3** form the same crystal structures as **1**.

The extended structure, as viewed down the *c*-axis, also contains dichloromethane molecules, which serve to occupy the void space and connect with host framework through van der Waals interactions to construct a stable architecture (Supporting Information).

Structure of **4**

Using the same experimental methods that produced **1–3**, we obtained the complex $0.5[\mathbf{L}\cdot 2\mathbf{H}]^{2+}\cdot 0.5[\text{Cu}_2\text{Br}_4]^{2-}\cdot \text{H}_2\text{O}$ (**4**) when mixing solution of CuBr_2 in MeOH and HBr/dichloromethane solution of **L**. The experimental PXRD suggests it is well matched with the simulated PXRD of **4** (Supporting Information). X-ray crystallography reveals that **4** crystallizes as a triclinic crystal system and the space group is *P*-1. Crystal **4** does not include MeOH or dichloromethane, but contains water molecules. Water molecules might come from the solvents (methanol or hydrobromic acid) we used in the preparation of crystals. The structure of **4** is significantly different from **1–3**. There are half doubly protonated **L**, half dinuclear anion $[\text{Cu}_2\text{Br}_4]^{2-}$, and one water in each asymmetric unit. The dinuclear anion $[\text{Cu}_2\text{Br}_4]^{2-}$ has two edge sharing planar configuration related by an inversion center. The Cu–Br terminal distance is 2.331(4) Å. The Cu–Br bridging distances are 2.167(4) and 2.242(3) Å, much shorter than the reported values of 2.39–2.45 Å for Cu–Br bridging distance. The Cu···Cu separation of 1.963(6) Å is also much shorter than the corresponding values for $[\text{Cu}_2\text{Br}_4]^{2-}$ reported in the literature, which are generally 2.30–2.77 Å [16]. This planar configuration of $[\text{Cu}_2\text{Br}_4]^{2-}$ is not common, with limited reports in the literature [16]. The unusually short Cu–Br distances might come from the direct N–H···Br interactions (3.268 Å) between **L** and $[\text{Cu}_2\text{Br}_4]^{2-}$. **L** and dinuclear anion are alternately arranged and form a chain along the *a*-axis. The water molecules are accommodated between neighboring chains along the *b*-axis, constructing a 3-D structure, as seen in figure 3.

Structure stability and thermal analysis

This new type of supramolecular complex was studied by thermogravimetric analysis. The thermogravimetry (TG) experiments for **1**, **3**, and **4** were performed under N_2 with a heating rate of $10\text{ }^\circ\text{C min}^{-1}$ from 25–800 °C, as shown in figure 4. For **1**, TGA curve exhibits an initial weight loss (15.40%) from 25 to 98 °C, corresponding to the release of CH_2Cl_2 and methanol (calcd 15.32%). The following weight loss at higher temperature results from decomposition of the complex. For **3**, an initial weight loss of 12.28% from 25 to 120 °C is assigned to the losses of CH_2Cl_2 and methanol molecules (calcd 12.87%), followed by structural collapse due to decomposition of complex at higher temperature. Crystal **4** shows a weight loss of 3.21% before 100 °C, corresponding to release of free water (calcd 3.26%). Further weight loss (9.25%) from 25 to 150 °C was considered as removal of HBr (calcd 9.86%) [17]. The subsequent weight loss at higher temperature is attributed to collapse of the complex.

According to TGA curves of **1** and **4**, the PXRD patterns have been recorded for **1** and **4** at high temperatures and then cooled to room temperature before testing. Dichloromethane molecules are prone to escape from the host framework if the sample was left in the air overnight, or heated, as **1** in 50 °C for 1 h (the crystal color are changed from dark blue to pale blue), which was confirmed by ^1H NMR (Supporting Information), suggesting the release of dichloromethane. PXRD patterns show that the positions and intensities of all peaks are changed, thus, the supramolecular host framework is changed since the solvents

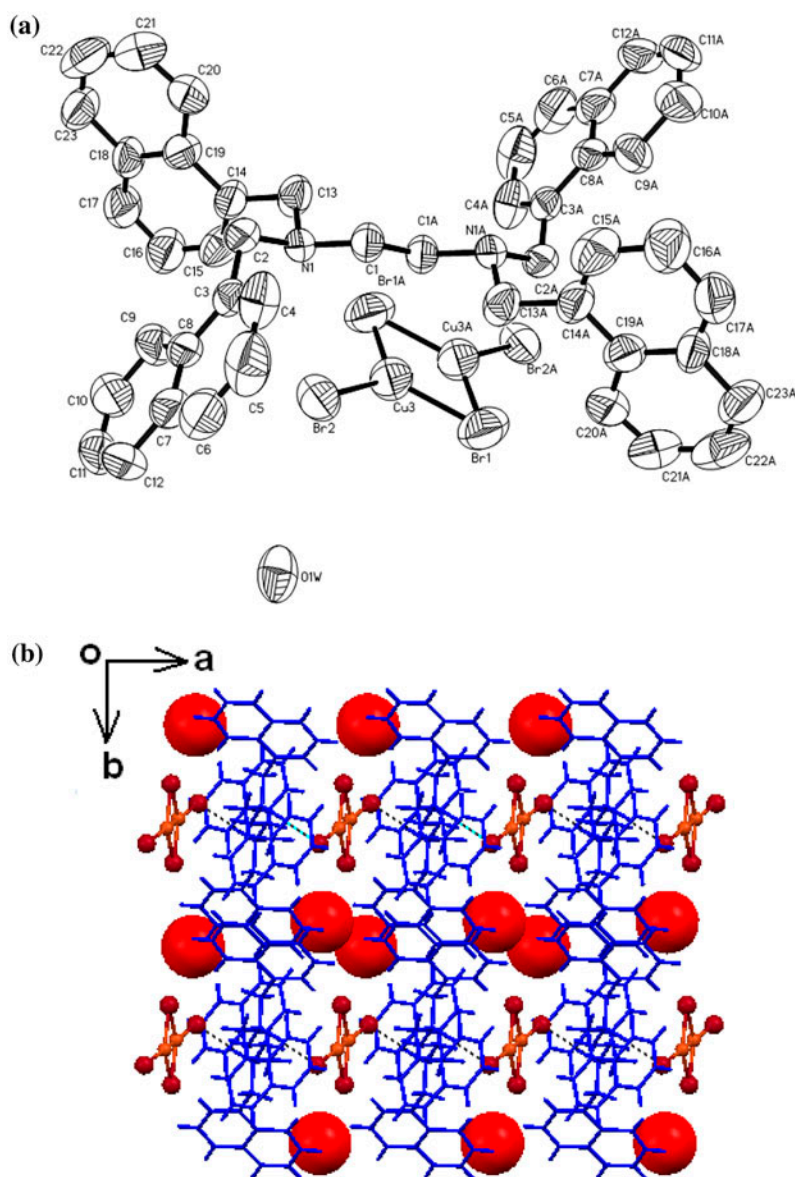


Figure 3. (a) The 30% probability ellipsoids in the ORTEPs for **4** showing dinuclear $[\text{Cu}_2\text{Br}_4]^{2-}$ and (b) Structural packing along the c -axis.

are removed. The easy loss of dichloromethane could arise from the weak interactions (only van der Waals force) between dichloromethane and host framework. When immersing the exposed sample into dichloromethane, the color changes back to transparent dark blue, suggesting the reabsorption of dichloromethane molecules, exhibiting a good reversible solvent/desolvation process [figure 5(a)].

According to TGA curves of **4**, water releases from the host framework before 100 °C. Thus, the sample of **4** was heated at 100 °C for 1 h and then the PXRD measurement was

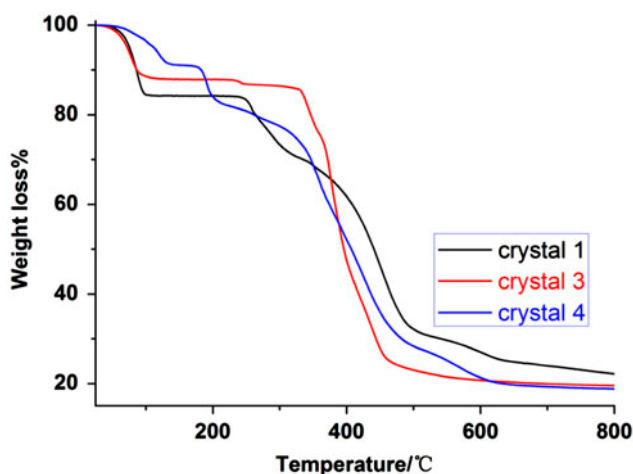


Figure 4. TGA of **1**, **3**, and **4**.

carried out. PXRD patterns showed the change of peak positions [figure 5(b)]. When dipping the heated sample into dichloromethane/methanol/HBr solvents for 1 d, the PXRD pattern changed back to the same PXRD of **4**. Thus, although **4** has different structural properties from **1** to **3**, **4** has a similar reversible solvent/desolvation process.

Effect of ligand upon second-sphere coordination with metal chloride

L exhibits slightly different conformations in **1–4**. The N···N distance is much elongated upon protonation and reaction with anions (**L**, 3.770 Å; **1**, 3.888 Å; **2**, 3.849 Å; **3**, 3.832 Å; **4**, 3.821 Å). The conformation difference of **L** in these crystals can be seen by viewing the ligand from the projection of the Newman-type overlay of two N and the dihedral angles between naphthalene rings attached to the same N (1/2 and 3/4) or different N (1/4, 2/3, and 1/3, 2/4) in figure 6 and table S1.

As a systematic study of supramolecular assemblies based on the second-sphere coordination strategy, we reported a series of complexes formed by N,N,N',N'-tetrabenzylethylenediamine (**L'**) [14, 15]. The only difference between **L** and **L'** is the benzene rings in **L'**, whereas the naphthyl rings in **L**, however, formed supramolecular architectures with $[\text{MCl}_4]^{2-}$ dianions and are distinct. Taking the complexes formed with $[\text{CoCl}_4]^{2-}$ as an example [18], **L** in **1–4** adopts mirror symmetry with both naphthalene rings attached to same N symmetrically oriented in both sides, with respect to the $(\text{CH}_2)_2$ chain (figure 6), whereas **L'** in $\text{CH}_3\text{CH}_2\text{OH} \text{C} [\text{H}_2\text{L}]^{2+} [\text{CoCl}_4]^{2-}$ is asymmetric, with the dihedral angles between benzene rings attached to same N being 109.56° and 120.82° , respectively [figure 6(f)]. Another significant difference lies in the hydrogen bond modes between protonated ligand and $[\text{CoCl}_4]^{2-}$: the chelating N–H···Cl interactions are the main driving force in $\text{CH}_3\text{OH} \text{C} [\text{H}_2\text{L}]^{2+} [\text{CoCl}_4]^{2-}$ [figure 6(g)], whereas the N–H···O (OH of methanol) and O–H (methanol)···Cl (Br) interactions with the help of the methanol as the linking bridge control the overall structural construction of **1–3**.

Most reported salts contain $[\text{MX}_4]^{2-}$ dianions and the organic N-containing compounds, such as protonated benzylamine and N-methylated derivatives [19(a)] or N-containing

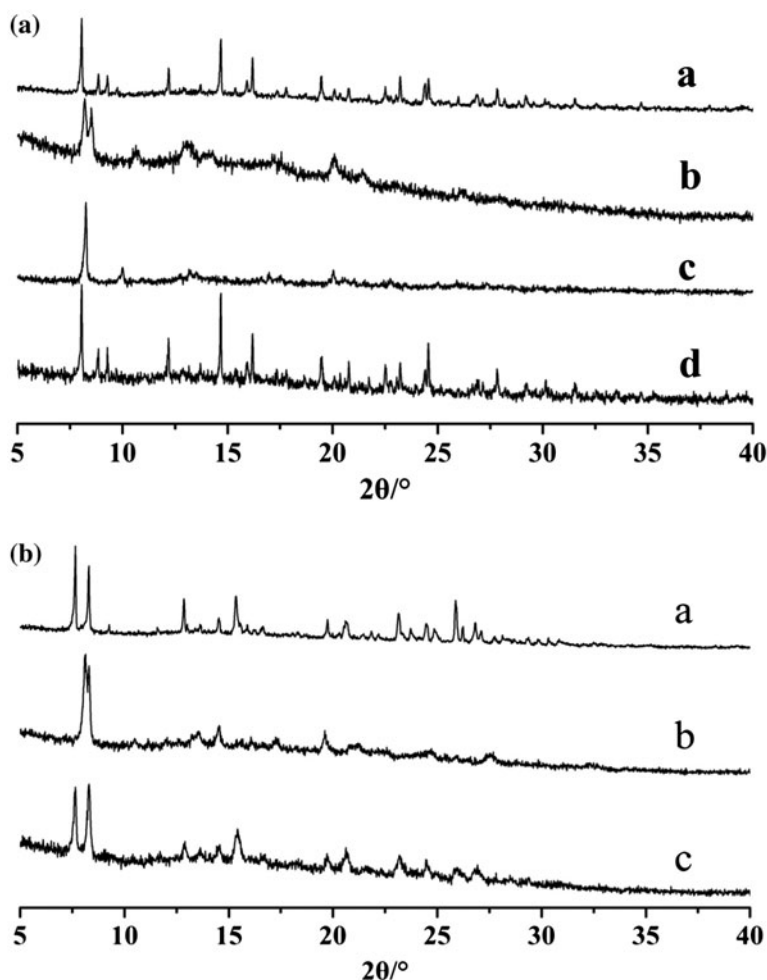


Figure 5. (a) a: PXRD of **1**, b: PXRD of **1** heated at 50 °C for 1 h, c: PXRD of **1** left in air overnight, d: PXRD of the heated sample dipped into the dichloromethane/methanol solvents and (b) a: PXRD of **4**, b: PXRD of **4** heated at 100 °C for 1 h, c: PXRD of the heated sample dipped into the dichloromethane/methanol solvents.

aromatic Brønsted bases [19(b)], and bis(benzimidazole)/bis(imidazole) derivatives [19(c)]. N–H···Cl (Br) interaction is without exception, the main driving force linking the organic and inorganic moiety. No involvement of N–H···Cl (Br) interactions in the presence of metal chloride and protonated N-containing organic ligands is rare.

*Photoluminescence “off–on” switch of **L** and its inclusion compounds*

Considering that the compounds containing naphthalene units commonly have fluorescent properties [20], we have investigated the photoluminescence properties of **L** and **1–4**. The fluorescence measurements indicate that **L** exhibits fluorescence (“on” state), with the maxima emission wavelength at 392 nm, as seen in figure 7. In the presence of the $[\text{MX}_4]^{2-}$

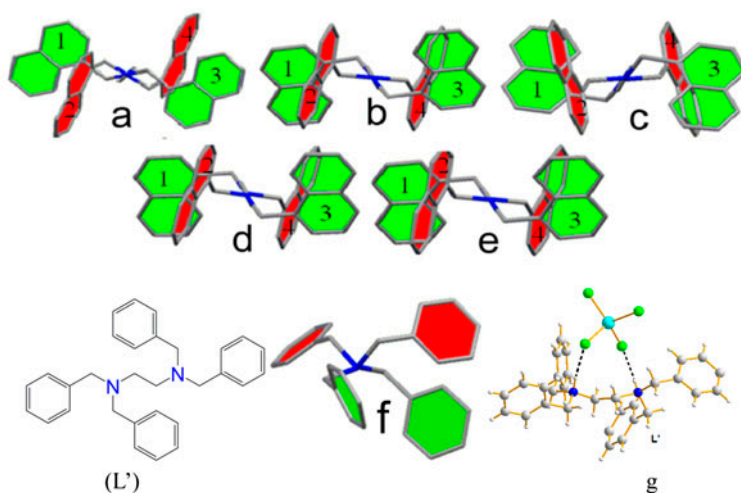


Figure 6. Newman-type overlay of two N atoms of **L**. Conformation of **L** in **1-4** (a-e) and **L'** in crystal $\text{CH}_3\text{OH C} [\text{H}_2\text{L}][\text{CoCl}_4]^{2-}$ (f). The chelating $\text{N-H}\cdots\text{Cl}$ interaction between **L'** and $[\text{CoCl}_4]^{2-}$ (g).

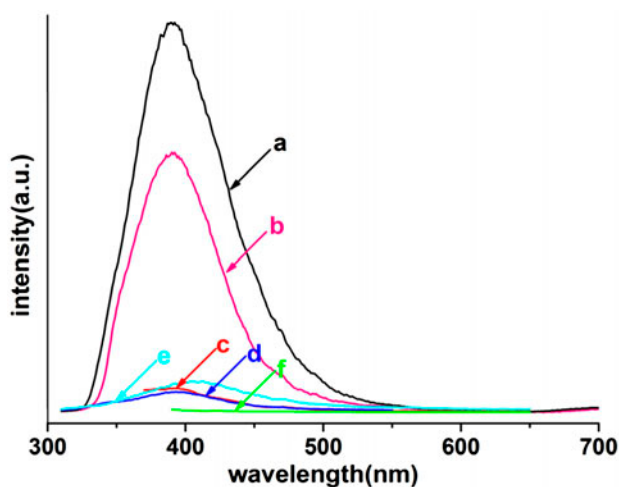


Figure 7. Fluorescent measurements of **L** and its inclusion complexes **1-4**. a: **L**, b: recrystallization of **1**, c: **1**, d: **2**, e: **3**, f: **4**.

template, the fluorescence measurements of **1-4** show significant decrease and even nearly zero excimer fluorescence (“off” state). Thus, the fluorescence measurement on ligand and its complexes with $[\text{MX}_4]^{2-}$ can be regarded as an “on-off” process.

Conclusion

In this article, we report four supramolecular complexes of $[\text{L}\cdot 2\text{H}]^{2+}\cdot[\text{MCl}_4]^{2-}\cdot[\text{CH}_3\text{OH}]\cdot 0.5[\text{CH}_2\text{Cl}_2]$ ($\text{M} = \text{Co}$, crystal **1**; $\text{M} = \text{Mn}$, crystal **2**), $[\text{L}\cdot 2\text{H}]^{2+}\cdot[\text{ZnBr}_4]^{2-}\cdot[\text{CH}_3\text{OH}]\cdot 0.5$

[CH₂Cl₂] (crystal **3**), and 0.5[L·2H]²⁺·0.5[Cu₂Br₄]²⁻·H₂O (crystal **4**). Crystals **1–4** are different from the complexes reported before, in which the N–H···Cl interactions connect the protonated ligand and [MCl₄]²⁻; in the present article, MeOH connects the protonated ligand and [MCl₄]²⁻ through N–H···O and O–H···Cl interactions into the host framework. An X-shaped channel was formed accessible for the inclusion of weakly polar guest molecules, such as dichloromethane. Dichloromethane is connected with the host framework through van der Waals force. The anions [MX₄]²⁻ acting as an “off-on” switching template control the photoluminescence.

Disclosure statement

No potential conflict of interest was reported by the authors.

Funding

This research was supported by the NSFC [grant number 20903052], [grant number 20772054]; the program for Liaoning excellent talents in University [LJQ 2011003]; the innovative team project of education department of Liaoning Province [LT2011001]; Liaoning university support [2012LDGY06].

References

- [1] (a) M.W. Hosseini. *Chem. Commun.*, 5825 (2005); (b) G.R. Desiraju. *Angew. Chem. Int. Ed.*, **46**, 8342 (2007).
- [2] G.R. Desiraju, J.J. Vittal, A. Ramanan. *Crystal Engineering*, World Scientific Publishing Company, Singapore (2011).
- [3] (a) S. Ferlay, W. Hosseini. *Chem. Commun.*, 788 (2004); (b) E.C. Constable. *Coord. Chem. Rev.*, **252**, 842 (2008); (c) M.J. Bojdys, M.E. Briggs, J.T.A. Jones, D.J. Adams, S.Y. Chong, M. Schmidtman, A.I. Cooper. *J. Am. Chem. Soc.*, **133**, 16566 (2011); (d) H.T. Black, D.F. Perepichka. *Angew. Chem. Int. Ed.*, **53**, 2138 (2014); (e) A. Bacch, M. Carcelli, P. Pelagatti. *Crystallogr. Rev.*, **18**, 253 (2012).
- [4] (a) J. Martí-Rujas, K.D.M. Harris, A. Desmedt, F. Guillaume. *J. Phys. Chem. B*, **110**, 10708 (2006); (b) J. Martí-Rujas, A. Desmedt, K.D.M. Harris, F. Guillaume. *J. Phys. Chem. C*, **113**, 736 (2009).
- [5] P. Vishweshwar, J.A. McMahon, M.L. Peterson, M.B. Hickey, T.R. Shattock, M.J. Zaworotko. *Chem. Commun.*, 4601 (2005).
- [6] (a) D.S. Reddy, S. Duncan, G.K.H. Shimizu. *Angew. Chem. Int. Ed.*, **42**, 1360 (2003); (b) S.A. Dalrymple, G.K.H. Shimizu. *J. Am. Chem. Soc.*, **129**, 12114 (2007).
- [7] A.N. Sokolov, T. Friščić, L.R. MacGillivray. *J. Am. Chem. Soc.*, **128**, 2806 (2006).
- [8] (a) S.A. Bourne, Z. Mangombo. *CrystEngComm*, **6**, 437 (2004); (b) G.M. Espallargas, J. Van de Streek, P. Fernandes, A.J. Florence, M. Brunelli, K. Shankland, L. Brammer. *Angew. Chem. Int. Ed.*, **49**, 8892 (2010); (c) M. Felloni, P. Hubberstey, C. Wilson, M. Schröder. *CrystEngComm*, **6**, 87 (2004); (d) D.K. Kumar, A. Ballabh, D.A. Jose, P. Dastidar, A. Das. *Cryst. Growth Des.*, **5**, 651 (2005).
- [9] (a) H.M. Colquhoun, D.F. Lewis, J.F. Stoddart, D.J. Williams. *Dalton Trans.*, **4**, 607 (1983); (b) H.M. Colquhoun, S.M. Doughty, J.F. Stoddart, D.J. Williams. *Angew. Chem. Int. Ed. Engl.*, **23**, 235 (1984).
- [10] (a) D.A.S. Beauchamp. *J. Loeb. Chem. Eur. J.*, **8**, 5084 (2002); (b) D.J. Mercer, S.J. Loeb. *Chem. Soc. Rev.*, **39**, 3612 (2010).
- [11] J.R. Turkington, V. Cocalia, K. Kendall, C.A. Morrison, P. Richardson, T. Sassi, P.A. Tasker, P.J. Bailey, K.C. Sole. *Inorg. Chem.*, **51**, 12805 (2012).
- [12] Z. Liu, M. Frasconi, J. Lei, Z.J. Brown, Z. Zhu, D. Cao, J. Iehl, G. Liu, A.C. Fahrenbach, O.K. Farha, J.T. Hupp, C.A. Mirkin, Y.Y. Botros, J.F. Stoddart. *Nat. Commun.*, **4**, 1855 (2013).
- [13] R. Zhang, Y.X. Zhao, J.M. Wang, L.G. Ji, X.J. Yang, B. Wu. *Cryst. Growth Des.*, **14**, 544 (2014).
- [14] (a) H.Y. Guan, Z. Wang, A. Famulari, X. Wang, F. Guo, J. Marti-Rujas. *Inorg. Chem.*, **53**, 7438 (2014); (b) F. Guo, H.D. Shao, Q. Yang, A. Famulari, J. Marti-Rujas. *CrystEngComm*, **16**, 969 (2014).
- [15] (a) F. Guo, F. Xia, H.Y. Guan, B.X. Wang, J. Tong, W.S. Guo. *Solid State Sci.*, **13**, 59 (2011); (b) F. Guo, M.Q. Zhang, N. Lu, J. Tong, H.Y. Guan, B.X. Wang. *CrystEngComm*, **13**, 6753 (2011); (c) F. Guo, S. Zhang, H.Y. Guan, W.S. Guo. *J. Coord. Chem.*, **67**, 1891 (2011); (d) F. Guo, L. Li, J. Tong, C.L. Song, F. Xia, W.S. Guo. *Supramol. Chem.*, **24**, 415 (2012); (e) L. Li, Y.Q. Fu, F. Guo, J. Gao, J. Tong, Z.F. Zhou. *RSC Adv.*, **3**, 11594 (2013).

- [16] (a) B. Gall, F. Conan, N. Cosquer, J. Kerbaol, M. Kubicki, E. Vigier, Y. Mest. *J. Pala. Inorg. Chim. Acta*, **324**, 300 (2001); (b) K. Kuro, H. Miyasaka, M. Yamashita. *Physica B*, **405**, S308 (2010); (c) A. Kapur, B. Ribar, M. Leovac, G. Argay, A. Kalman, S.Y. Chundak. *J. Coord. Chem.*, **38**, 139 (1996); (d) S. Andersson, S. Jagner. *Acta Cryst.*, **C43**, 1089 (1987).
- [17] C.J. Adams, H.M. Colquhoun, P.C. Crawford, M. Lusi, A.G. Orpen. *Angew. Chem. Int. Ed.*, **46**, 1124 (2007).
- [18] L. Yuan, F. Guo, S. Zhang, Z.Q. Hu, F. Xia, W.S. Guo. *Chem. J. Chin. Univ.*, **10**, 1897 (2007).
- [19] (a) Y. Jin, C.H. Yu, W. Zhang. *J. Coord. Chem.*, **67**, 1156 (2014); (b) S.W. Jin, D.Q. Wang. *J. Coord. Chem.*, **65**, 3188 (2012); (c) J.M. Pan, Q. Wei, J.X. Ju, B. Liu, S.W. Jin, Z.H. Lin, D.Q. Wang. *J. Coord. Chem.*, **67**, 3578 (2014).
- [20] (a) X.J. Wang, L.C. Gui, Q.L. Ni, Y.F. Liao, X.F. Jiang, L.H. Tang, Z. Zhang, Q. Wu. *CrystEngComm*, **10**, 1003 (2008); (b) I.S. Tidmarsh, T.B. Faust, H. Adams, L.P. Harding, L. Russo, W. Clegg, M.D. Ward. *J. Am. Chem. Soc.*, **130**, 15167 (2008); (c) F. Tuna, J. Hamblin, G. Clarkson, W. Errington, N.W. Alcock, M.J. Hannon. *Chem. Eur. J.*, **8**, 4957 (2002); (d) L. Fang, S. Basu, C.H. Sue, A.C. Fahrenbach, J.F. Stoddart. *J. Am. Chem. Soc.*, **133**, 396 (2011).